

**Table S1.** Main crystallographic data for the crystal of complex **1**.

Empirical formula	C <sub>42</sub> H <sub>54</sub> Cl <sub>6</sub> N <sub>2</sub> O <sub>14</sub> Dy <sub>2</sub> ( <b>1</b> )
Formula weight	1348.56
Temperature	100.00(10) K
Wavelength	0.7107 Å
Crystal system, space group	Monoclinic, P 21/c
a, Å	10.3832(4)
b, Å	18.1959(10)
c, Å	13.7949(4)
alpha, deg.	90
beta, deg.	92.590(3)
gamma, deg.	90
Volume	2603.63(19) Å <sup>3</sup>
Z, Calculated density	4, 1.720 Mg/m <sup>3</sup>
Absorption coefficient	3.217 mm <sup>-1</sup>
F(000)	1332
Crystal size	0.10 x 0.05 x 0.02 mm
Theta range for data collection	2.956 to 26.069 deg.
Limiting indices	-12<=h<=12, -15<=k<=22, -17<=l<=9
Reflections collected / unique	10218 / 5131 [R(int) = 0.0742]
Completeness to theta	25.242 99.8 %
Absorption correction	Semi-empirical from equivalents
Max. and min. transmission	1.00000 and 0.54734
Refinement method	Full-matrix least-squares on F <sup>2</sup>
Data / restraints / parameters	5131 / 12 / 298
Goodness-of-fit on F <sup>2</sup>	0.818
Final R indices [I>2sigma(I)]	R1 = 0.0503, wR2 = 0.0734
R indices (all data)	R1 = 0.1010, wR2 = 0.0921
Extinction coefficient	n/a
Largest diff. peak and hole	1.604 and -1.334 e.Å <sup>-3</sup>

**Table S2.** Selected bond lengths and valence angles in complex **1**.

Bond	d, Å	Bond	d, Å
Dy(1)-O(2)	2.312(4)	Dy(1)-O(5)	2.360(5)
Dy(1)-O(4)	2.321(5)	Dy(1)-O(7)#1	2.425(5)
Dy(1)-O(1)	2.335(5)	Dy(1)-O(7)	2.514(5)
Dy(1)-O(3)	2.340(5)	Dy(1)-O(6)	2.313(5)
Угол	ω, degree	Угол	ω, degree
O(6)-Dy(1)-O(2)	141.30(18)	O(3)-Dy(1)-O(5)	75.70(17)
O(6)-Dy(1)-O(4)	76.94(17)	O(6)-Dy(1)-O(7)#1	92.75(17)
O(2)-Dy(1)-O(4)	73.75(18)	O(2)-Dy(1)-O(7)#1	90.70(16)
O(6)-Dy(1)-O(1)	145.88(16)	O(4)-Dy(1)-O(7)#1	135.36(18)
O(2)-Dy(1)-O(1)	72.48(16)	O(1)-Dy(1)-O(7)#1	79.43(17)
O(4)-Dy(1)-O(1)	130.88(17)	O(3)-Dy(1)-O(7)#1	151.38(17)
O(6)-Dy(1)-O(3)	92.77(17)	O(5)-Dy(1)-O(7)#1	79.17(17)
O(2)-Dy(1)-O(3)	102.21(17)	O(6)-Dy(1)-O(7)	74.26(16)
O(4)-Dy(1)-O(3)	73.18(19)	O(2)-Dy(1)-O(7)	74.10(16)
O(1)-Dy(1)-O(3)	80.31(18)	O(4)-Dy(1)-O(7)	74.85(17)
O(6)-Dy(1)-O(5)	72.89(17)	O(1)-Dy(1)-O(7)	126.62(16)
O(2)-Dy(1)-O(5)	145.27(17)	O(3)-Dy(1)-O(7)	147.48(17)
O(4)-Dy(1)-O(5)	134.97(18)	O(5)-Dy(1)-O(7)	125.72(15)
O(1)-Dy(1)-O(5)	73.03(16)	O(7)#1-Dy(1)-O(7)	60.60(19)

**Table S3.** The local symmetry of Dy(III) ions for **1** defined by the continuous shape measure (CShM) analysis with SHAPE 2.1 software [54].

			Structure	CShM
1	D <sub>8h</sub>	OP-8	Octagon	32.054
2	C <sub>7v</sub>	HPY-8	Heptagonal pyramid	24.336
3	D <sub>6h</sub>	HBPY-8	Hexagonal bipyramid	16.100
4	O <sub>h</sub>	CU-8	Cube	9.942
5	D <sub>4d</sub>	SAPR-8	Square antiprism	2.529
<b>6</b>	<b>D<sub>2d</sub></b>	<b>TDD-8</b>	<b>Triangular dodecahedron</b>	<b>0.492</b>
7	D <sub>2d</sub>	JGBF-8	Johnson gyrobifastigium J26	13.453
8	D <sub>3h</sub>	JETBPY-8	Johnson elongated triangular bipyramid J14	29.524
9	C <sub>2v</sub>	JBTPR-8	Biaugmented trigonal prism J50	2.623
10	C <sub>2v</sub>	BTPR-8	Biaugmented trigonal prism	2.183
11	D <sub>2d</sub>	JSD-8	Snub diphendoid J84	2.802
12	T <sub>d</sub>	TT-8	Triakis tetrahedron	10.614
13	D <sub>3h</sub>	ETBPY-8	Elongated trigonal bipyramid	24.076

**Table S4.** SINGLE\_ANISO computed wave function decomposition analysis for the lowest KDs of Dy(III) ion in **1**. Only main contributions (>10%) are shown

KD	RASSI wave function composition
<b>1</b>	<b>0.945</b>   $\pm 15/2$ $\rangle$
<b>2</b>	<b>0.795</b>   $\pm 13/2$ $\rangle$ +0.176   $\pm 9/2$ $\rangle$
<b>3</b>	<b>0.225</b>   $\pm 11/2$ $\rangle$ + 0.211   $\pm 1/2$ $\rangle$ + 0.207   $\pm 3/2$ $\rangle$ + 0.175   $\pm 7/2$ $\rangle$ + 0.125   $\pm 5/2$ $\rangle$
<b>4</b>	<b>0.266</b>   $\pm 11/2$ $\rangle$ + 0.265   $\pm 1/2$ $\rangle$ +0.233   $\pm 7/2$ $\rangle$ +0.124   $\pm 3/2$ $\rangle$
<b>5</b>	<b>0.388</b>   $\pm 5/2$ $\rangle$ + 0.272   $\pm 3/2$ $\rangle$ +0.148   $\pm 1/2$ $\rangle$ + 0.119  $\pm 9/2$ $\rangle$
<b>6</b>	<b>0.298</b>   $\pm 9/2$ $\rangle$ +0.234   $\pm 7/2$ $\rangle$ +0.195   $\pm 11/2$ $\rangle$
<b>7</b>	<b>0.276</b>   $\pm 1/2$ $\rangle$ + 0.256   $\pm 3/2$ $\rangle$ +0.132   $\pm 9/2$ $\rangle$ + 0.122   $\pm 5/2$ $\rangle$ +0.102   $\pm 11/2$ $\rangle$
<b>8</b>	<b>0.274</b>   $\pm 7/2$ $\rangle$ +0.223   $\pm 9/2$ $\rangle$ +0.186   $\pm 5/2$ $\rangle$ + 0.124  $\pm 11/2$ $\rangle$

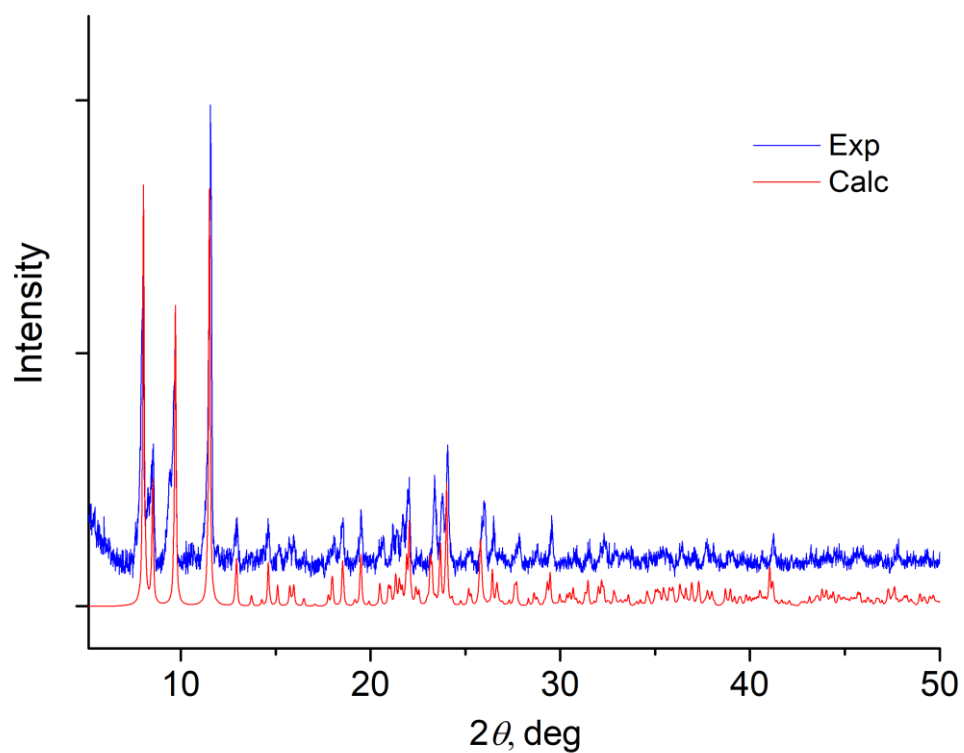


**Figure S1.** Powder X-ray diffraction pattern of polycrystalline sample of **1**: experimental (blue), and calculated from single crystal data (red).

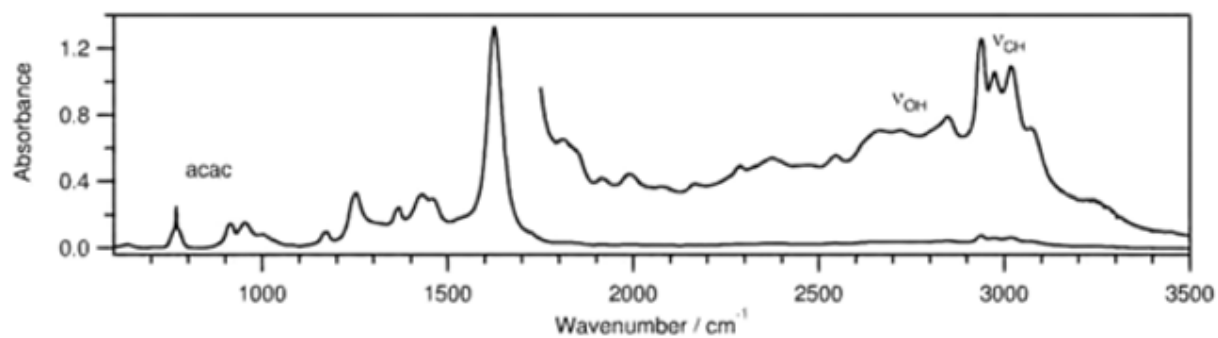


**Figure S2.** Experimental IR spectrum of acac **Error! Reference source not found.**

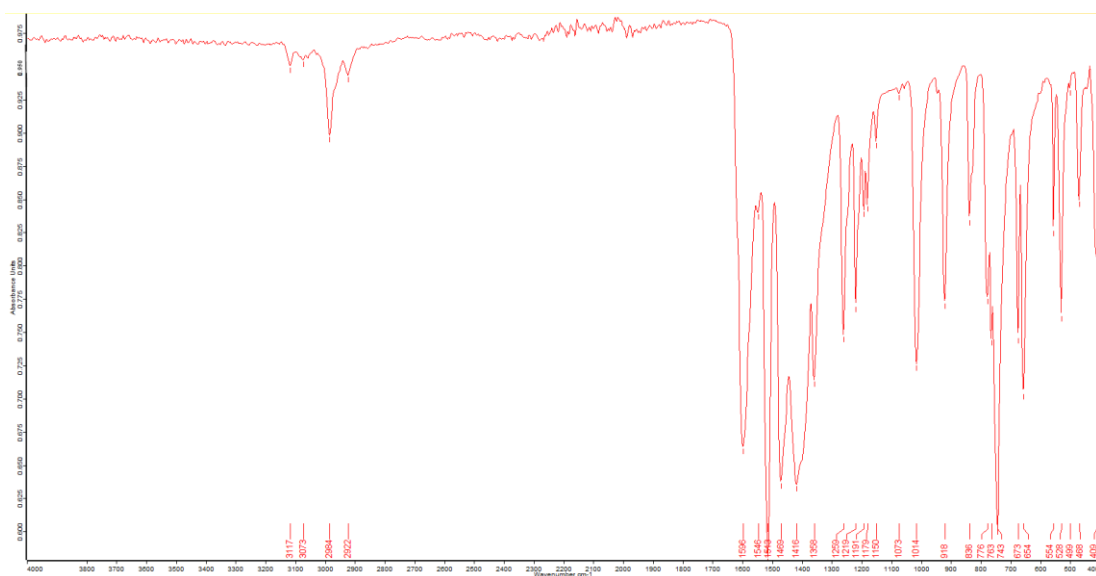


**Figure S3.** Experimental IR spectrum of **1**.

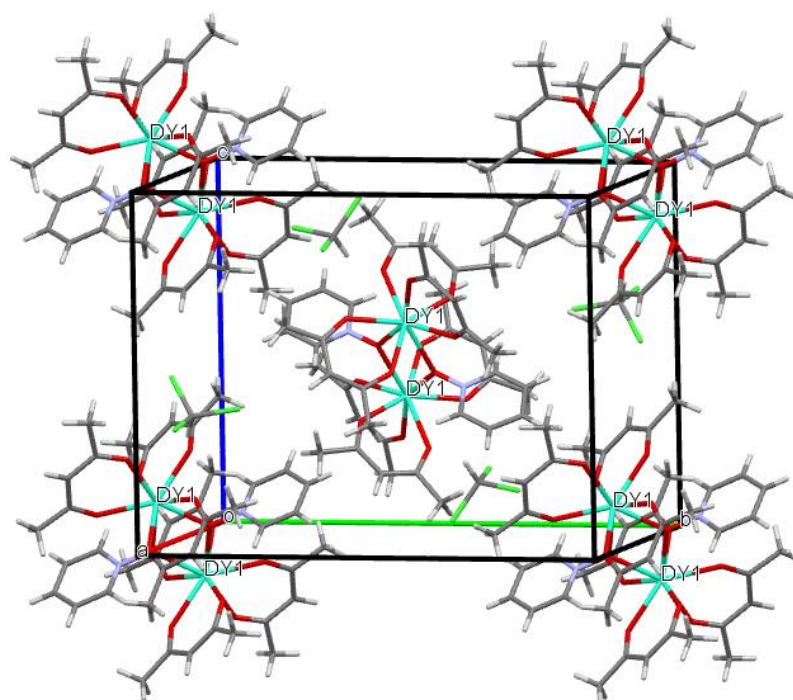


**Figure S4.** Crystalline packing of **1**.

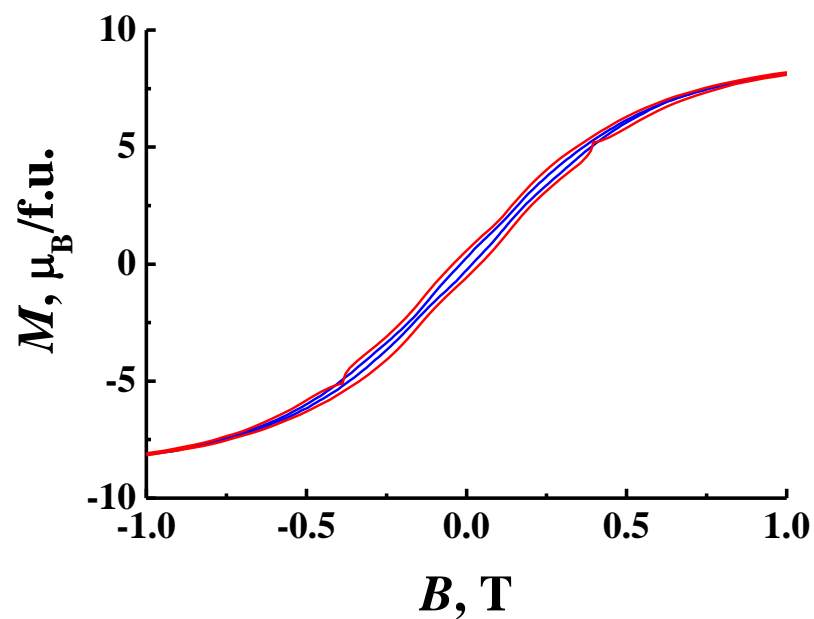


**Figure S5.** Magnetic hysteresis loops at 2 K with magnetic field sweep rates of 0.3 T/min (blue line) and 0.9 T/min (red line).

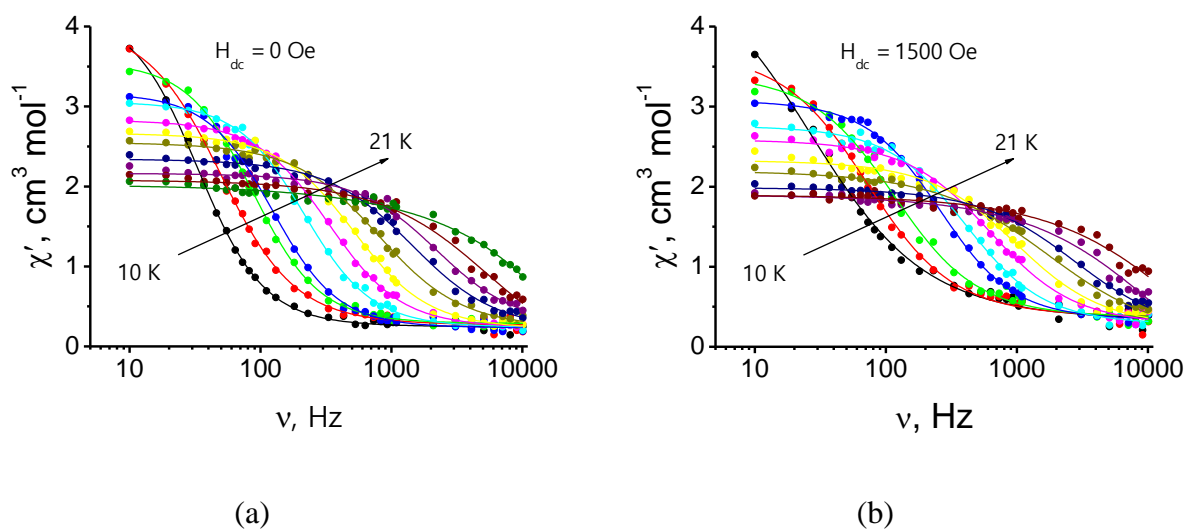


**Figure S6.** Frequency dependences of the in-phase ac susceptibility signals for complex 1 at zero (a) and 1500 Oe (b) dc fields and temperatures from 10 to 21 K.

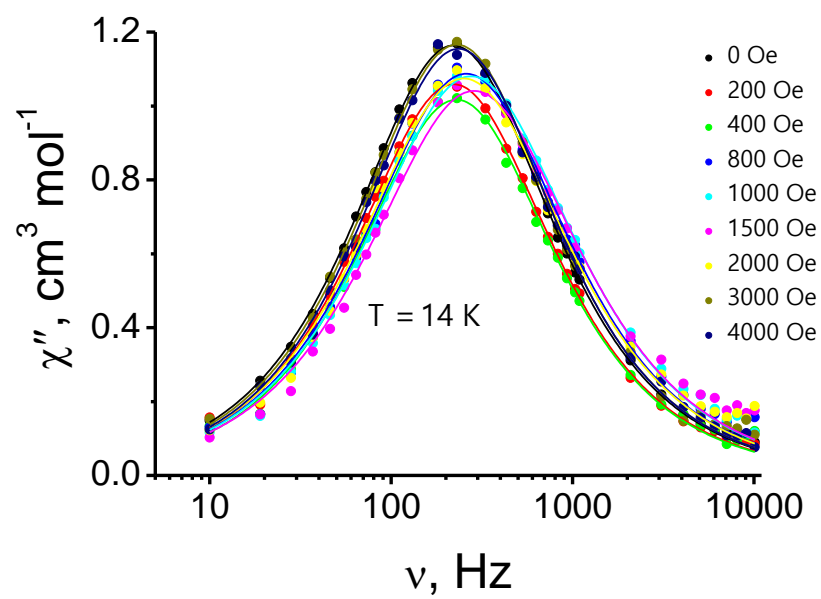


**Figure S7.** Frequency dependences of the out-of-phase ac susceptibility for **1** at temperature 14 K and applied dc fields from 0 to 4000 Oe.